Physical Chemistry Chemical Physics b800519b

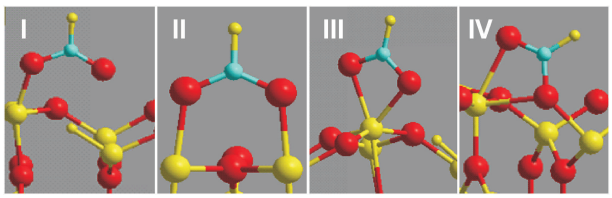

Q1 **Stability of formate species on β-Ga_2O_3**

M. Calatayud, S. E. Collins, M. A. Baltanás and A. L. Bonivardi

Formate species are formed on a gallia surface by CO insertion in hydroxyl groups.

Please check this proof carefully. **Our staff will not read it in detail after you have returned it.** Translation errors between word-processor files and typesetting systems can occur so the whole proof needs to be read. Please pay particular attention to: tabulated material; equations; numerical data; figures and graphics; and references. If you have not already indicated the corresponding author(s) please mark their name(s) with an asterisk. Please e-mail a list of corrections or the PDF with electronic notes attached -- do not change the text within the PDF file or send a revised manuscript.

Please bear in mind that minor layout improvements, e.g. in line breaking, table widths and graphic placement, are routinely applied to the final version.

Please note that, in the typefaces we use, an italic vee looks like this: v, and a Greek nu looks like this: ν.

We will publish articles on the web as soon as possible after receiving your corrections; **no late corrections will be made.**

Please return your **final** corrections, where possible within **48 hours** of receipt, by e-mail to: proofs@rsc.org

Reprints—Electronic (PDF) reprints will be provided free of charge to the corresponding author. Enquiries about purchasing paper reprints should be addressed via: http://www.rsc.org/Publishing/ReSourCe/PaperReprints/. Costs for reprints are below:

Reprint costs		
No of pages	Cost for 50 copies	Cost for each additional 50 copies
2-4	£190	£120
5-8	£315	£230
9-20	£630	£500
21-40	£1155	£915
>40	£1785	£1525
Cost for including cover of journal issue: £55 per 50 copies		

Queries are marked on your proof like this Q1, Q2, etc. and for your convenience line numbers are indicated like this 5, 10, 15, ...

Query reference	**Query**	**Remarks**
Q1	For your information: You can cite this article before you receive notification of the page numbers by using the following format: (authors), Phys. Chem. Chem. Phys., 2009, DOI: 10.1039/b800519b.	
Q2	Affiliation b. Please provide the full postal address.	
Q3	'...reverse WGS reaction...' Please define WGS in the text. Is it water gas shift?	
Q4	'...because no hydrogen (or deuterium) bond is involved on CO3^--...' I have changed the = to a minus sign in the superscript. If the = is correct, please give a definition in the text.	
Q5	Ref. 7. Please give the type of thesis - I have put PhD provisionally.	

Stability of formate species on β-Ga_2O_3

M. Calatayud,*[a] S. E. Collins,[b] M. A. Baltanás[b] and A. L. Bonivardi[b]

Received 10th January 2008, Accepted 25th November 2008
First published as an Advance Article on the web
DOI: 10.1039/b800519b

Gallia (gallium oxide) has been proved to enhance the performance of metal catalysts in a variety of catalytic reactions involving methanol, CO and H_2. The presence of formate species as key intermediates in some of these reactions has been reported, although their role is still a matter of debate. In this work, a combined theoretical and experimental approach has been carried out in order to characterize the formation of such formate species over the gallium oxide surface. Infrared spectroscopy experiments of CO adsorption over H_2 (or D_2) pretreated β-Ga_2O_3 revealed the formation of several formate species. The β-Ga_2O_3 (100) surface was modelled by means of periodic DFT calculations. The stability of said species and their vibrational mode assignments are discussed together with the formate interconversion barriers. A possible mechanism is proposed based on the experimental and theoretical results: first CO inserts into surface (monocoordinate) hydroxyl groups leading to monocoordinate formate; this species might evolve to the thermodynamically most stable dicoordinate formate, or might transfer hydrogen to the surface oxidizing to CO_2 creating an oxygen vacancy and a hydride group. The barrier for the first step, CO insertion, is calculated to be significantly higher than that of the monocoordinate formate conversion steps. Monocoordinate formates are thus short-lived intermediates playing a key role in the CO oxidation reaction, while bidentate formates are mainly spectators.

Introduction

Hydrogen production for energy-related purposes is a major task in catalysis nowadays. One of the most promising processes for hydrogen production is steam reforming from methanol (SRM): $CH_3OH + H_2O \rightarrow 3\,H_2 + CO_2$.[1,2] However, methanol decomposition occurs alongside with the main reaction and it is responsible for the production of CO in the system.

Both the SRM reaction and its reverse, methanol synthesis from H_2 and CO_2, can be efficiently accomplished over palladium–gallium oxide (gallia)-based catalysts.[3,4]

The mechanisms for methanol decomposition and methanol production from CO_2 have been studied by some of us.[5,6] The key intermediate in these two reactions was proposed to be the formate surface species ($HCOO^-$), which can be either decomposed to carbonate and Ga–H to finally desorb as CO_2 and H_2, or be hydrogenated stepwise to methylenebisoxy, methoxy and methanol.[5,6] It was suggested as well that the presence of gallium oxide also favours the reverse WGS reaction ($CO + H_2O \rightarrow CO_2 + H_2$) *via* formate intermediates.[7]

However, several formate species coexist or can be formed under reaction conditions, and some of them suffer interconversion.[5] The role of formate species as potential reaction intermediates in the WGS reaction has been the subject of a renewed debate in the recent literature. The main work has been focused on noble metal catalysts supported on ceria. Two main reaction mechanisms have been proposed for the WGS reaction over these ceria-based materials:[8,9] (i) a redox mechanism, where CO(g) adsorbs on metal sites to form a carbonyl species, which then reacts with an oxygen atom coming from the ceria to form CO_2 (the reduced ceria is subsequently reoxidized by water and hydrogen is produced as a result), as follows:

$$CO + O_{Lattice} \rightarrow CO_2 + \square \quad (\square\text{: oxygen vacancy})$$

$$\square + H_2O \rightarrow H_2 + O_{Lattice};$$

and (ii) a non-redox mechanism, where it was concluded that the main reaction intermediate is a bidentate formate produced by reaction of CO with terminal hydroxyl groups on the ceria surface (this formate species was thought to decompose into H_2(g) and CO_2(g) *via* surface carbonate groups), as summarized in the following steps:

$$CO + OH \rightarrow HCOO + O_{Lattice}$$

$$HCOO \rightarrow \tfrac{1}{2}H_2 + CO_2 + \square$$

$$H_2O + \square \rightarrow OH + \tfrac{1}{2}H_2.$$

Based on DRIFTS analyses combined with the utilization of isotopic tracers, Meunier's group showed, on a Pt/CeO_2 catalyst, that formates were less reactive than carbonyl and carbonate species under steady-state conditions.[8] More recently, the same research group concluded, from the analysis of the formate exchange curves between 428 and 493 K, that at least two levels of reactivity were present.[10,11] "Slow formates" displayed an exchange rate 10- to 20-fold slower than that of

[a] *Laboratoire de Chimie Théorique, UMR 7616 CNRS, Boîte 137 site Ivry, Université Pierre et Marie Curie, 4 Place Jussieu Paris, 75252 cedex 05, France. E-mail: calatayu@lct.jussieu.fr; Fax: +33 (1)44 27 41 17; Tel: +33 (1)44 27 26 82*
[b] *Instituto de Desarrollo Tecnológico para la Industria Química (CONICET-UNL), Argentina*

the reaction product, CO_2, and "fast formates" which were exchanged on a time scale similar to that of CO_2. However, a discussion taking into consideration the presence of different types of surface formate groups is so far absent in those pictures.

Thus, it seems clear that many aspects regarding the structure and reactivity of formates are still not well understood, in particular their role as intermediates, or spectators, in the WGS reaction. For this reason we have performed a combined theoretical and experimental investigation of the stability of formate species on the pure Ga_2O_3 surface. We have focused on the characterization of the adsorption mode and the relative stability of the different types of formates obtained from the reaction: $CO + O_{Lattice}H^- \rightarrow HCOO^-$. A possible mechanism for formates interconversion and oxidation to CO_2 is proposed based on the experimental findings and the calculated reaction barriers.

Methodology

Computational details

The Perdew–Burke–Ernzerhof functional has been used to compute total energy calculations as implemented in the VASP code.[12,13] The core electrons are kept frozen and replaced by projector augmented wave generated (PAW) pseudopotentials while the valence electrons are described with a plane-wave basis set (cutoff = 400 eV). The valence electrons explicitly treated are the following O: s^2p^4, Ga: s^2p^1, C: s^2p^2, H: s^1. A $3 \times 3 \times 1$ Monkhorst–Pack sampling in the Brillouin zone is used; this scheme gives converged total energies within 0.010 eV, and surface energies within 0.005 J m^{-2}. Geometry optimizations are carried out with the conjugate-gradient algorithm. Harmonic frequencies were calculated with the finite differences method as implemented in VASP; the structures are checked to be minima in the potential energy hypersurface. The reaction barriers for interconversion of different species are determined by constrained optimization algorithms (nudged elastic band, NEB) as implemented in the code.[14]

The (100) surface is thermodynamically the most stable plane of the β-Ga_2O_3 crystal structure;[15] it has been modelled by a slab containing 4 Ga_2O_3 layers (see Fig. 1). The surface is terminated by tetrahedral Ga_t, uncoordinated octahedral Gacus, and three-fold oxygen O_{3f} atoms. A 2×1 unit cell is employed, with dimensions $6.00 \times 5.75 \times 20$ Å^3, leaving a vacuum layer of ~10 Å between successive slabs. For the structure characterization all the atoms are allowed to relax; for the transition states only the uppermost 2 Ga_2O_3 layers together with the adsorbate are allowed to relax. The surface is terminated by tetrahedral Ga_t, coordinatively unsaturated octahedral Ga_{cus}, and three-fold oxygen O_{3f} atoms.

Experimental details

β-Ga_2O_3 phase, with a Brunauer–Emmett–Teller surface area equal to 64 m^2 g^{-1}, was synthesized following the procedure previously reported by some of us. A self-supported wafer of the gallia sample was placed into an infrared Pyrex® cell with water-cooled NaCl windows, which was attached to a conventional manifold system. After an *in situ* cleaning pretreatment of the wafer (heating under O_2 up to 723 K), the sample was activated at 723 K by flowing H_2 (or D_2) through the cell at atmospheric pressure, then cooling down to 298 K under vacuum. Next, pure CO (100 cm^3 min^{-1}) was admitted into the IR cell and the temperature was increased from 298 to 723 K. All the treatments were done at 0.1 MPa. *In situ* infrared spectra were taken using a Shimadzu 8210 FT-IR spectrometer employing a deuterated L-alanine doped tri-glycine sulfate (DLATGS) detector.

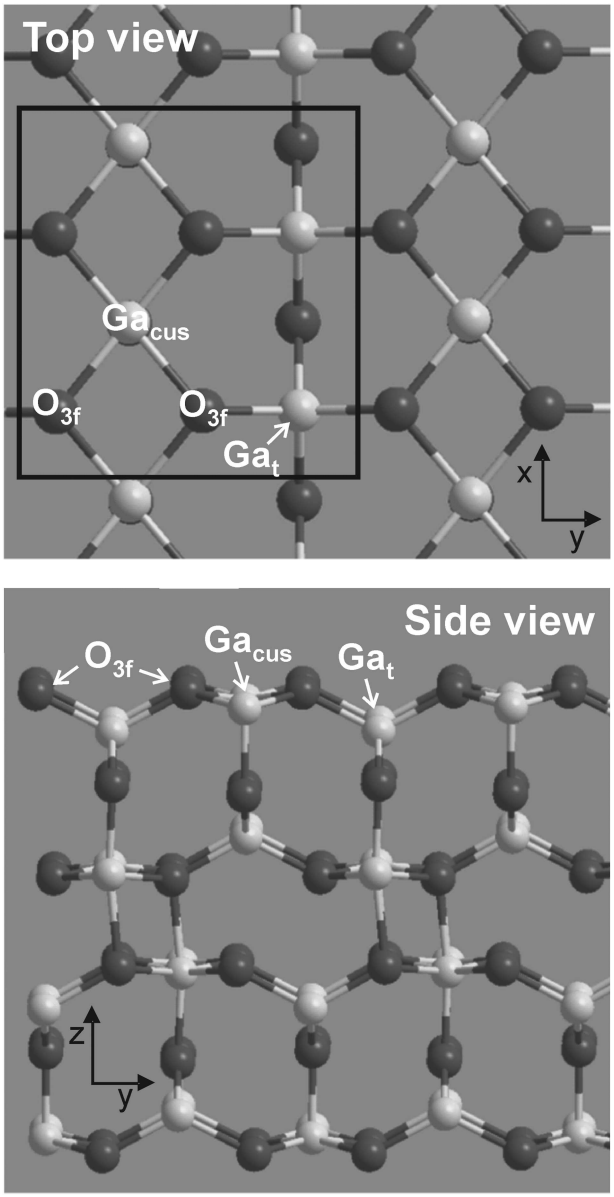

Fig. 1 The slab model used in the calculations. Coordinatively unsaturated octahedral Ga_{cus}, tetrahedral Ga_t and three-fold oxygen O_{3f} atoms are exposed on the (100) β-Ga_2O_3 surface.

Results and discussion

A suitable analysis regarding formate(s) formation on the gallia surface can be done by considering CO adsorption

and reactivity. The adsorption of CO on a bare, dehydroxylated Ga_2O_3 surface is found to be very weak: it is not detected in experiments and the energy stabilization is calculated to be of 0.02 eV. Conversely, formate species are generated by CO insertion on OH surface groups on a wide range of hydroxylated metal oxides (for example, ZnO, Al_2O_3, TiO_2, V_2O_5, Fe_2O_3, ZrO_2 and CeO_2[16–19]). The formation and decomposition of $HCOO^-$ species on gallium oxide proceeds as shown in the following scheme:

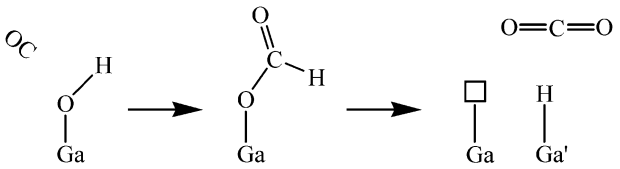

The first step involves the insertion of CO in the OH bond leading to the formation of a formate species. This reaction proceeds without electron transfer and needs the presence of a hydroxyl group. Subsequent steps involve the oxidation to CO_2 and its desorption, leaving an oxygen vacancy on the surface.

We have focused on the characterization of the formate species coming from the CO insertion in the OH group. The presence of hydride and hydroxyl groups has been detected in IR experiments after H_2 adsorption.[20] Such pairs H^-/H^+ are stabilized on irreducible metal oxide surfaces (MgO, ZnO), at variance to reducible transition metal oxides (TiO_2, V_2O_5) where no hydride but only hydroxyl groups are found after hydrogenation.[21,22]

Computational modelling

The system considering formal adsorption of H_2 as H^-/Ga_{cus} + H^+/O_{3f} has been modelled. The calculated adsorption energy is −2.25 eV, indicating an exothermic process with respect to atomic hydrogen. At this stage we did not consider terminal or bridging hydroxyl groups that can be originated at defects or through a different mechanism. The 2 × 1 unit cell is shown in Fig. 2: it contains two Ga_{cus}, one of them capped by a H atom, and a O_{3f}–H group, together with Ga_{cus} and O_{3f} available for reactivity.

Carbon monoxide insertion in the OH bond was considered, leading to four formate structures which are shown in Fig. 3.

The insertion of CO in the OH bond is exothermic for all the structures. The most stable system is II, which corresponds to a dicoordinate formate, stabilized by the formation of two Ga–O bonds. The adsorption energy with respect to CO and the hydrogenated surface is −0.82 eV. Structure IV is 0.32 eV less stable in energy; it corresponds to the insertion of CO into the lattice O_{3f}–H group. Structure I is a monodentate formate that could be formed by rearrangement of structure IV: the lattice oxygen is abstracted and the hydride tilts to occupy the vacancy. Structure III involves a dicoordinate formate bonded to one gallium site; it is 0.47 eV less favourable than the dicoordinate formate II and evolves to the latter upon optimization. Note that a hydride species is always present in the models, in some cases occupying a lattice oxygen vacancy (I, II and III). The barriers for the interconversion of such formate species are calculated and discussed below.

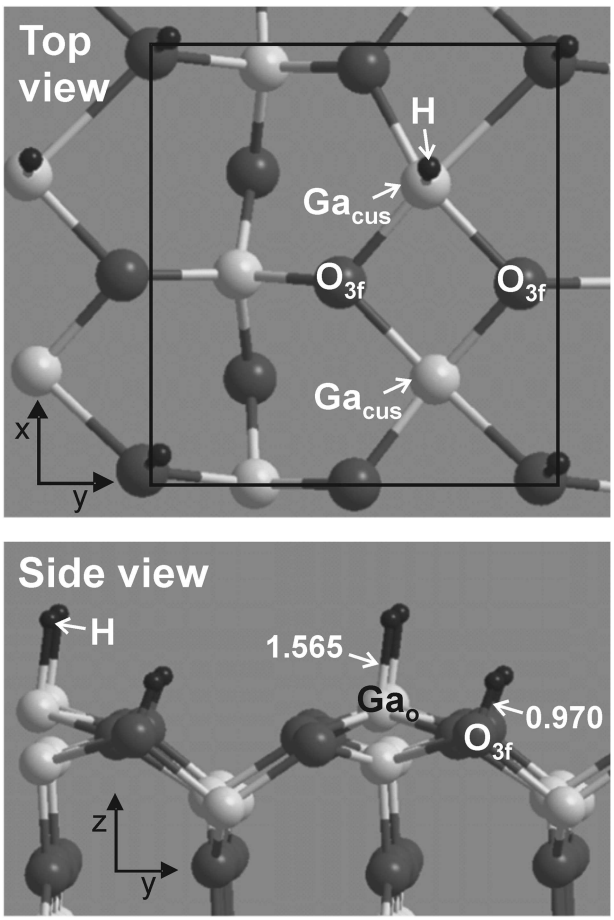

Fig. 2 Hydrogenated slab model. After H_2 adsorption Ga–H and O–H groups are formed. Uncoordinated Ga_{cus} and three-fold oxygen O_{3f} atoms are exposed, Ga_o stands for a H-capped Ga_{cus}.

The harmonic frequencies calculated for the four structures are reported in Table 1 (see next section for experimental data). The calculation of intensities is not implemented in the code. The formate stretching modes are located around 1600 cm^{-1} (COO asymmetric) and 1300 cm^{-1} (COO symmetric). The vibrations around 3000 cm^{-1} and 1300 cm^{-1} are assigned to the C–H stretching and bending modes, respectively. Hydride groups (Ga–H) are found to vibrate at values of 1900 cm^{-1}, that is at 100 cm^{-1} lower than the experimental value (~2000 cm^{-1}),[20] which is found for metal-H frequencies calculated by DFT.[23]

Infrared spectroscopy

Because the spectra in the hydroxyl IR region (3700–3000 cm^{-1}) were opaque, by the interference of gaseous water from the environment (*i.e.* outside the IR cell), the Fig. 4 shows the infrared spectra during the temperature-programmed adsorption of CO (101.3 kPa) on β-Ga_2O_3 previously activated under molecular deuterium. The IR spectra show that, as the intensity of the OD bands (at 2800–2600 cm^{-1}) decreased from 448 K, new overlapped bands developed in the 1700–1300 cm^{-1} region. The same spectroscopic behaviour was observed

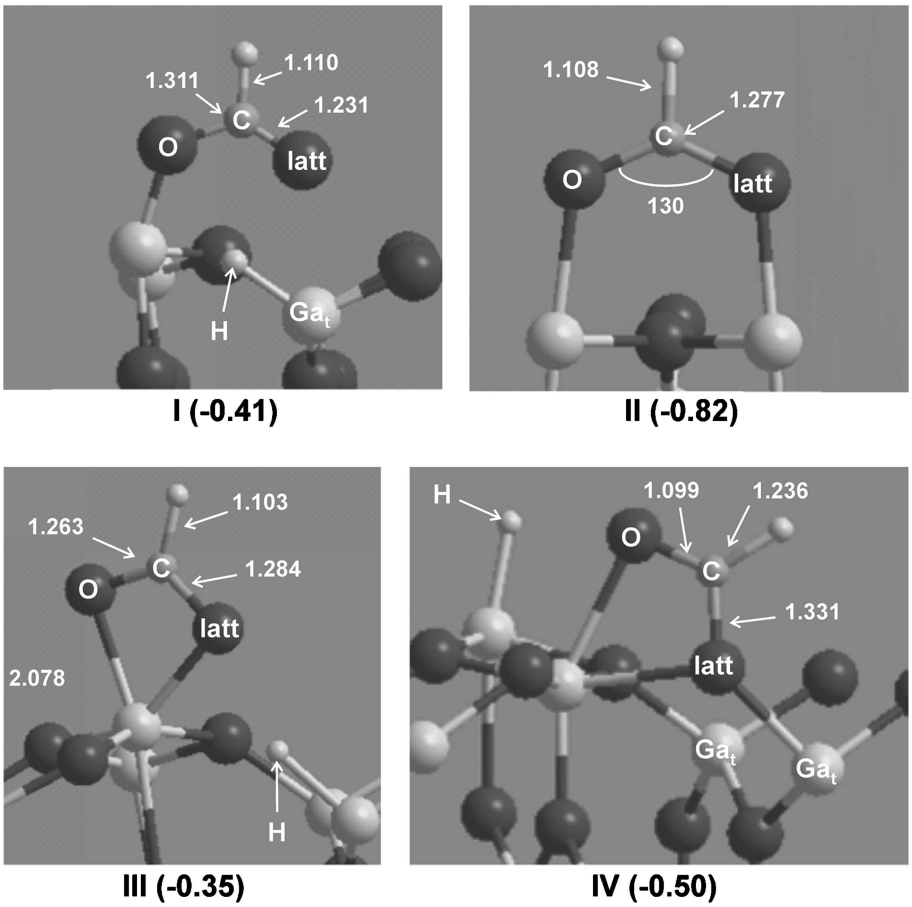

Fig. 3 Different formate groups calculated over the β-Ga_2O_3 (100) surface: mono- (I), di- (II and III), and tri-coordinate (IV) species. Between parentheses, the relative energy with respect to CO + Ga_2O_3–H_2, in eV; latt stands for lattice oxygen.

Table 1 Calculated and experimental harmonic frequencies for the formate ($HCOO^-$) species

	Infrared frequencies of formate species/cm^{-1}							
	I		II		III		IV	
Vibrational mode	Calcd	Exptl[a]	Calcd	Exptl[a]	Calcd	Exptl[a]	Calcd	Exptl[a]
C–H stretching	2923	2910	2973	2915	3011	2895	3062	n.d.
COO asym stretching (ν_{as})	1634	1665	1538	1580	1581	1600	1624	n.d.
C–H bending	1341	1350	1354	1385	1250	1355	1294	n.d.
COO sym stretching (ν_s)	1252	1305	1310	1369	1324	1332	1187	n.d.
$\Delta\nu = \nu_{as} - \nu_s$	382	360	228	211	257	268	437	—

[a] Average values obtained from the whole set of IR spectra between 448 and 723 K, during the temperature-programmed adsorption of pure CO (100 cm^3 min^{-1}, 0.1 MPa) over a β-Ga_2O_3 sample previously activated in H_2 (see the experimental section for operational details). n.d.: not detected.

over the hydrogen-activated β-Ga_2O_3 (that is, gallium oxide activated under H_2) upon due consideration, vis-à-vis the isotopic shifting of the respective bands. A detail of the IR spectra at 623 K, that is at the highest total surface formate concentration (mainly type II and III formates, see below), together with the partial assignments of the vibrational modes of $HCOO^-$ ($DCOO^-$) and Ga–H (Ga–D) groups on the gallia surface are shown in Fig. 5.

The position and relative intensity of the new set of bands in the 1700–1300 cm^{-1} region refers to formate groups as follows: the most intense bands at approximately 1600 and 1330 cm^{-1} correspond to the asymmetric and symmetric stretching mode of the COO group [ν_{as}(COO) and ν_s(COO)], respectively, of the $HCOO^-$ species.[5] It is clear that these bands shifted no more than −30 cm^{-1} for the deuterated formate species (Fig. 5).[5] Meanwhile, the bending mode of the CH group [δ(CH)], which showed up at approximately 1360 cm^{-1}, was strongly affected by the isotopic exchange and shifted to 993 cm^{-1} (not shown), that is, by a factor of 1.37, in agreement with the expected theoretical ratio of 1.36 [$\delta(CH)/\delta(CD) = (\mu_{CD}/\mu_{CH})^{1/2}$, where μ_{CD} and μ_{CH} are the reduced masses of CD and CH, respectively].[5] Simultaneously, two weak bands

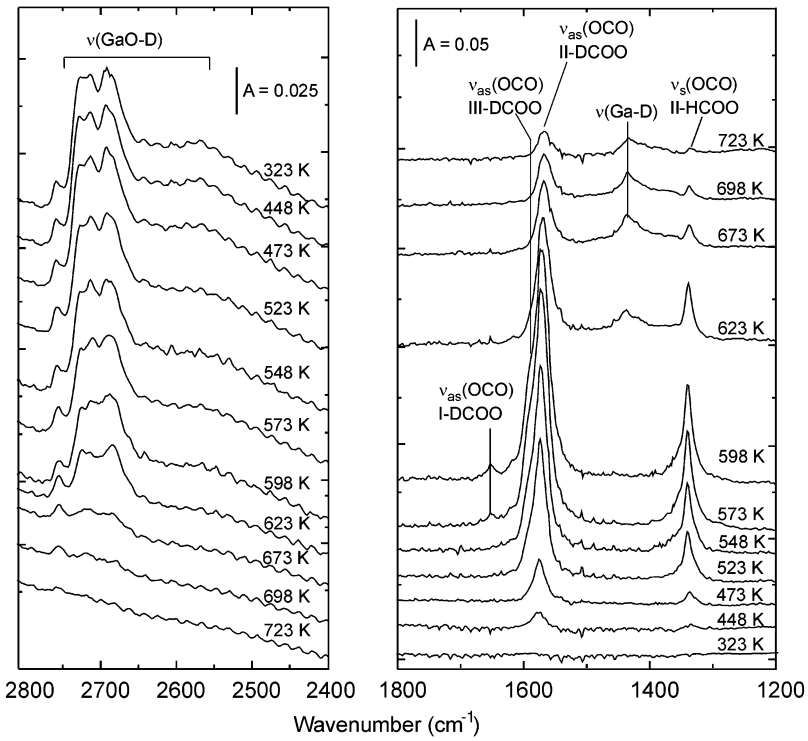

Fig. 4 Thermal evolution of the IR spectra during the CO adsorption (760 Torr CO) over a β-Ga_2O_3 surface activated under D_2 at 723 K. (Background subtraction: clean wafer at each temperature, under vacuum.)

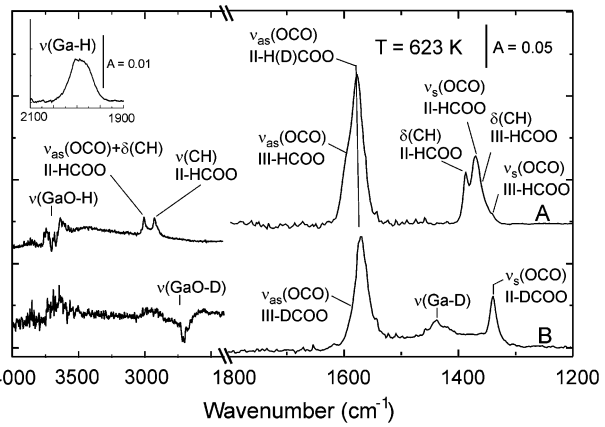

Fig. 5 IR spectra of adsorbed $HCOO^-$ ($DCOO^-$) and Ga–H (Ga–D) groups on β-Ga_2O_3 activated in H_2 (A) or D_2 (B), upon CO adsorption (760 Torr CO) at 623 K.

assigned to the ν(CH) [$\sim$2900 cm^{-1}] and the combination of the ν_{as}(COO) + δ(CH) modes, were also noticeable in the spectrum obtained at high surface formate concentration (see Fig. 5). Yet, the isotopic shifting in this last two cases could not be measured under the temperature programmed CO adsorption experiments because of the very low intensity of the ν_{as}(COO) + δ(CD) signal, and the overlapping between the ν(CD) peak and the ν(CO) band of $DCOO^-$ and gaseous CO, respectively.

It should be notice that (bi)carbonate species were not detected under our experimental conditions. In a deep infrared study of the carbon dioxide adsorption of different gallium oxide polymorphs, some of us have shown that (bi)carbonate groups develop several bands in the 1800–1200 cm^{-1} region.[24] However, those (bi)carbonates were really unstable, that is, only polydentate carbonates is still present under vacuum (base pressure = 10^{-6} Torr) but they decompose under heating (>373 K). Moreover, carbonate groups should not show any isotopic shifting after reacting CO with OD surface species, because no hydrogen (or deuterium) bond is involved on CO_3^-. Thus, this is a further piece of evidence that the bands observed in the 1700–1300 cm^{-1} region do not belong to carbonate groups.

Then, it is evident that more than one peak for each infrared mode of formate are present in the spectra, which means that $HCOO^-$ groups with different coordination coexist on the gallia surface. Certainly, the distinction among these different surface coordination formate species is not an easy task owing to the IR signal overlapping. Fig. 6 shows a correlation chart, which was built by compiling the experimental IR signals of different formate species over several metal oxides and organometallic complexes.[16–18,25–41] According to Busca and Lorenzelli,[17] formate species can be distinguished from each other by the band splitting of the asymmetric and symmetric COO stretching modes [$\Delta\nu$(COO) = ν_{as}(COO) − ν_s(COO)]. After comparing the frequency location of the ν_{as}(COO) and ν_s(COO) of formate metallic complexes whose structures were determined by X-ray diffraction, it was possible to establish the following $\Delta\nu$(COO) progression for the monodentate (type I), bidentate (type III) and dicoordinate (type II) formate species, respectively: type I > type III ≥ type II.[17] In our case, and computing the $\Delta\nu$(COO) from *average* ν(COO) values, this last trend is identical: 291 cm^{-1} (type I) > 223 cm^{-1} (type III) > 208 cm^{-1} (type II). However, the range of

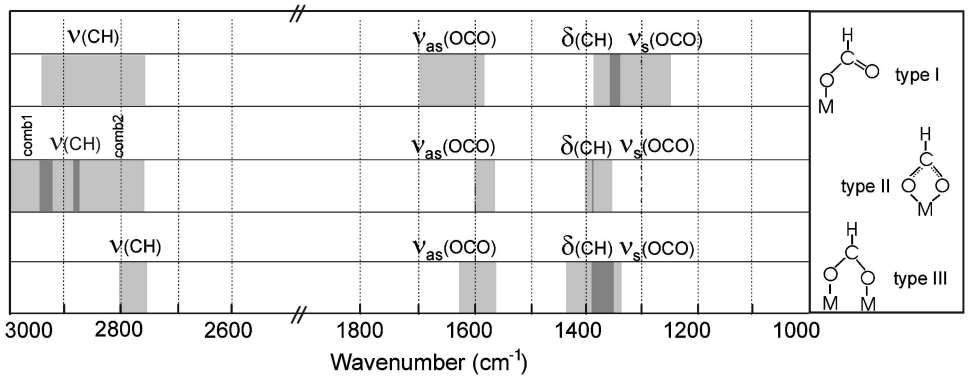

Fig. 6 Experimental IR vibrational frequency correlation chart of different types of formate species over several metal oxides and organometallic complexes [comb1 stands for ν_{as}(COO) + δ(CH) and comb2 stands for ν_s(COO) + δ(CH)]. The compiled data correspond to monodentate (type I), dicoordinate (type II) and bidentate (type III) formate species.[17–19,23–39] The light-grey regions indicate the range for the reported vibrational frequencies, while the dark-grey regions correspond to the overlapping between two neighbour light-grey regions, that is, between two vibrational modes of the same type of formate.

positions of the ν_{as}(COO) and ν_s(COO) bands for all of these three types of formate are overlapped (see Fig. 6), and a clear-cut discernment among them is very difficult from experimental data alone (that is, by merely comparing reported experimental band positions and/or performing isotopic exchange experiments). Even more, some of us have misinterpreted the bidentate formate IR signal in the past.[5,6] The theoretical calculation of the vibrational frequencies by DFT presented here sheds additional light on the assignment of formate species. Thence, the calculation makes it possible to discriminate among type I, II and III formates on gallium oxide, as presented on Table 1.

The different surface formate species (mainly, types II and III, and traces of type I) reached a maximum at approximately 573 K (see Fig. 4), where a band attributed to the Ga–D stretching mode showed up [ν(Ga–D) = 1430 cm^{-1}][20] and increased its intensity up to 698 K. However: (i) type I species could only be detected in a short range of temperature (573–598 K), and (ii) at the highest temperature, that is 723 K, only the type II formate species remains over the gallia surface.

At 623 K type I formate is no longer detected and (assuming similar extinction coefficients) a much smaller amount of formate III is still present, as compared to the type II species (see Fig. 5). That is, similar stability of type I and III formates is observed, being the formate II the most stable species. The inset in Fig. 6 displays—after subtracting the intense band of gaseous CO—the Ga–H stretching signal at approximately 2000 cm^{-1}, in accordance with previous results.[20] The experimental ratio of the ν(Ga–H)/ν(Ga–D) frequencies was equal to 1.39, in agreement with the expected theoretical ratio of 1.40 for the H–D isotopic exchange of Ga–H species.[20]

Therefore, these results suggest that CO reacts with the surface OH groups towards formate species with different thermal stability, being the dicoordinate (type II) formate the most stable oxycarbonaceous species. So, in an effort to improve the picture about the coexistence and the band assignment of the different types of formate species, an extra IR experiment was run by feeding the IR cell with a flowing mixture of CO_2 and H_2 (H_2/CO_2 = 3, 140 cm^3 min^{-1}) at 0.1 MPa, that is, under reverse water gas shift reaction conditions ($CO_2 + H_2 = CO + H_2O$). The β-gallia sample was activated under O_2 and H_2, as previously described in the experimental section. Next, the temperature-programmed reverse WGS reaction was studied over the β-gallium oxide wafer using H_2/CO_2 = 3. Under these experimental conditions the best signal-to-noise ratio for the monodentate formate was achieved at 573 K. Fig. 7 shows the IR spectrum of the formate region and the complete assignment of the vibrational modes of type I, II and III formates *only in one spectrum* (spectrum A). For comparison purposes spectrum B, corresponding to the CO adsorption on gallia at the same temperature, is also included.

It is reasonable to conclude, then, that the measured IR frequencies for the different formate species are in good

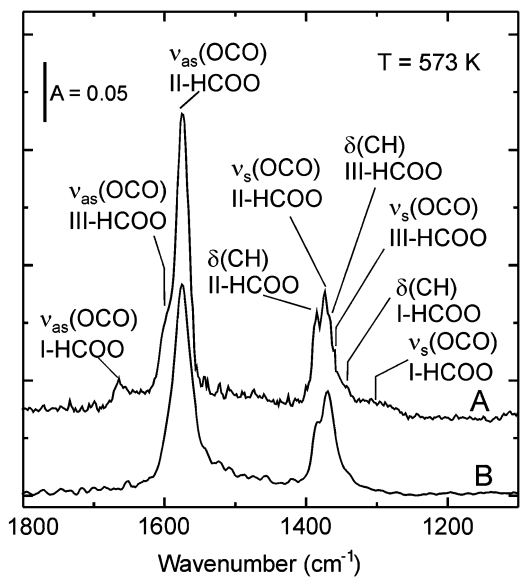

Fig. 7 IR spectra of formate species I, II, and III at 573 K on β-Ga_2O_3 (activated in H_2 at 723 K): (A) under a flowing mixture of hydrogen and carbon dioxide (H_2/CO_2 = 3, 140 cm^3 min^{-1}; 0.1 MPa); (B) upon CO adsorption (760 Torr CO).

agreement with those predicted by the DFT calculations (Table 1).

Nevertheless, no experimental evidence for the tricoordinate (type IV) formate was found under any of the experimental conditions employed here, which confirms that formate IV is the most unstable species on the gallia surface.

Truly, some reaction intermediates are usually difficult to be found due to their low concentration, low stability and/or high reactivity, while spectators (namely, stable and/or not active species) are frequently observed instead, and sometimes erroneously assumed as true reaction intermediates.[42,43] As a consequence, relevant catalytic and kinetic information may escape spectral 'capture', and inappropriate spectral interpretation might be conducive to deficient reaction pathways. In our case, for instance (and to circumvent this frequent hurdle), it is apparent that the evolution of surface formate species must be followed by using the IR signals in the 1700–1300 cm^{-1} region instead of the C–H stretching region, where no distinction among formate groups can be performed whatsoever.

Formate interconversion

The barriers for the interconversion of the different formate species have been calculated. A reaction path connecting the different structures has been constructed for the hydrogenated model, and is shown in Fig. 8.

The first step is the CO insertion into the surface OH group leading to the three-fold coordinated formate (species IV). The barrier calculated for the corresponding transition state is 2.11 eV. Next, the formate evolves to monocoordinated (species I) by the abstraction of lattice oxygen, the vacancy being filled by the hydride group. The H atom is now closer to the Ga_t site, leaving a Ga_{cus}. The barrier for this process is 0.77 eV. Structure I could then rotate and form any of the dicoordinated formates II (dicoordinate) or III (bidentate). We were not able to find a saddle point for such processes; if it existed it would be (in either case) lower in energy than the other barriers involving breaking/forming bonds. Monocoordinated formate could then oxidize to CO_2 by an H-transfer to a lattice oxygen.

The calculated barrier of 2.11 eV found for the CO insertion into the surface OH group is indeed very high. This might be due to the coordination of the surface hydroxyl group, which is three-fold in the model used. For the sake of completeness we have calculated the barriers in a model containing a monodentate hydroxyl group. The model used is equivalent to the hydrogenated model (Fig. 2) where the hydride group is replaced by an OH group, which is formally a water molecule dissociated as $OH^-/Ga_{cus} + H^+/O_{3f}$. The corresponding reaction paths and energy diagrams are displayed in Fig. 9. The energy barrier for the CO insertion into this singly coordinated hydroxyl group is 1.78 eV, which is significantly lower than the value obtained for the three-fold coordinated one. This indicates that the CO insertion process takes place on the terminal hydroxyl groups rather than on the many-fold coordinated. The so-formed monocoordinate formate, I-bis, is stabilized by a hydrogen bond to the surface. The subsequent conversion to the most stable dicoordinate formate II-bis takes place through a barrier of 0.54 eV. We have also calculated the barrier for the oxidation of the monocoordinate formate to CO_2, which is 0.82 eV. This process occurs *via* the hydrogen transfer to a surface gallium site forming a hydride group and a surface oxygen vacancy.

According to these results, the rate-limiting step is the insertion of CO in the surface hydroxyl group. The high barrier explains the absence of reaction between CO and gallia

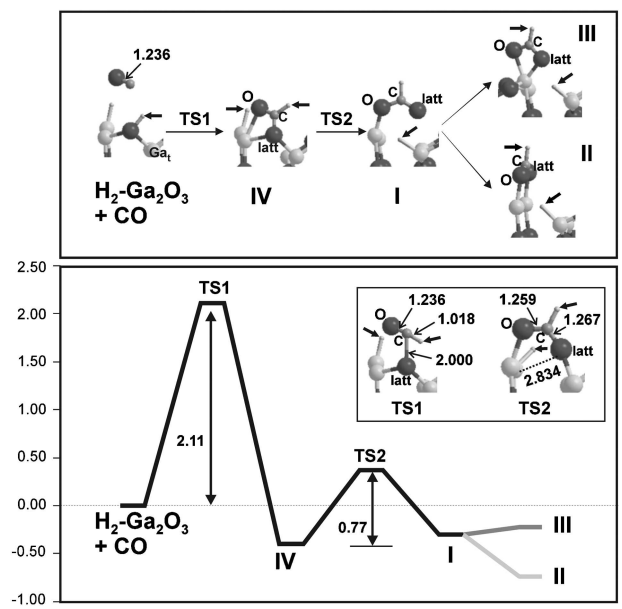

Fig. 8 Reaction path for the interconversion of the different formate species (see Fig. 3), barriers in eV. Inset: transition state structures, distances in Å. Hydrogen atoms are indicated with a thick arrow. O_{latt}: lattice oxygen, Ga_t: tetrahedral site.

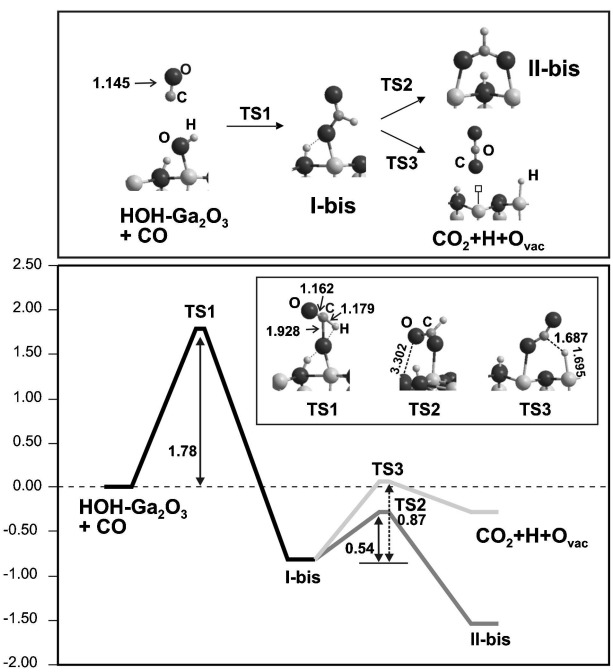

Fig. 9 Reaction path for the interconversion/decomposition of the different formate species on a monocoordinate hydroxyl-covered surface (HOH–Ga_2O_3), barriers in eV. Inset: transition state structures, distances in Å. O_{vac}: oxygen vacancy.

at low temperatures, as it was observed experimentally. Once this barrier is overcome, the evolution to a monodentate formate takes place. Further conversion to dicoordinate formates proceeds with a significantly lower barrier to species III (isoenergetic), and species II and II-bis (the most stable). Infrared experiments indicate the presence of both species II and III, which are accumulated up to high temperatures. The low intensity of the IR bands assigned to species I can be explained by the rapid transformation to the most stable species, type II. Therefore, the monodentate formates are short-lived intermediates due to (i) a high activation energy for their formation and (ii) a lower barrier for intercorversion/decomposition to CO_2. This behaviour has been observed in other metal oxides (see for instance ref. 44).

However, type II species disappear at higher temperatures. This might be due to the conversion to species I and subsequent oxidation to CO_2. The monocoordinate formate would then be the key reaction intermediate in the CO oxidation while dicoordinated formates would mainly be spectators. The monocoordinate formates II would ultimately be consumed by transformation to monocoordinate I and further oxidation.

Note that the calculated barriers, even considering monocoordinated surface hydroxyl groups, are high (1.78 eV). Experimentally it is observed the formation of formates at 200 C, which would correspond to lower barriers. This disagreement might be due to the presence of more reactive hydroxyl groups (as in defects, nests or more reactive surfaces). Also, the calculated values could be overestimated by the DFT method used: it is known that the values of energetic barriers strongly depend on the exchange–correlation functionals employed. Overall, the mechanism proposed, despite the high values found for the CO insertion step, is coherent with the observed data.

Conclusions

The interaction of CO with surface hydroxyl groups leads to the formation of stable formate species as confirmed by infrared spectroscopy and periodic DFT calculations. The dicoordinate formate bonded to two uncoordinated gallium sites is found to be the most stable species. The corresponding IR vibrations of the formate species have been calculated and compared to experimental assignments with good agreement. A possible mechanism for formate interconversion and oxidation to CO_2 is proposed based on the experimental data and calculated energetic barriers. The first step consists in the CO insertion into a surface OH group leading to a monocoordinate formate, with a barrier of 1.78 eV for a monocoordinate hydroxyl species. Next, the monocoordinate formate rotates to form a bidentate formate which is the most stable species. This process is associated to a calculated barrier of 0.54 eV. The monodentate formate may also oxidize to CO_2 with a hydrogen transfer to a surface gallium site, forming a hydride group and an oxygen vacancy. The calculated barrier for this process is 0.82 eV. This mechanism explains the observed trends in IR experiments: formation of formates at 200 °C (the insertion of CO into hydroxyl groups possesses the highest calculated barrier and is the rate limiting step), type II formates accumulate (and are assigned to dicoordinate species) at higher temperatures, at 673 K the signal disappears (dicoordinate species reconvert to monocoordinate and oxidize to CO_2) and a Ga–H band appears (hydride groups are formed by H-transfer from monocoordinate formate to gallium surface sites). The monocoordinate formate would thus be a short-lived intermediate in the oxidation of CO in agreement with the small signal observed in the IR spectra, while dicoordinate species would be mainly spectators.

Acknowledgements

Computational facilities by IDRIS, CINES and CCRE are acknowledged. SEC, MAB and ALB acknowledge the financial support of the CONICET and ANPCyT of Argentina.

References

1. L. Carrette, K. A. Friedrich and U. Stimming, *Fuel Cells*, 2001, **1**, 5.
2. B. Lindström and L. J. Pettersson, *J. Power Sources*, 2003, **118**, 71.
3. A. L. Bonivardi, D. L. Chiavassa, C. A. Querini and M. A. Baltanás, *Stud. Surf. Sci. Catal.*, 2000, **130D**, 3747.
4. N. Iwasa, T. Mayanagi, W. Nomura, M. Arai and N. Takezawa, *Appl. Catal. A: General*, 2003, **248**, 153.
5. S. E. Collins, M. A. Baltanas and A. L. Bonivardi, *J. Catal.*, 2004, **226**, 410.
6. S. E. Collins, M. A. Baltanas and A. L. Bonivardi, *Appl. Catal. A: General*, 2005, **295**, 126.
7. S. E. Collins, PhD Thesis, Universidad Nacional del Litoral, 2005. Q5
8. A. Goguet, F. C. Meunier, D. Tibiletti, J. P. Breen and R. Burch, *J. Phys. Chem. B*, 2004, **108**, 20240.
9. D. Tibiletti, A. Goguet, F. C. Meunier, J. P. Breen and R. Burch, *Chem. Commun.*, 2004, 1636.
10. F. C. Meunier, D. Reida, A. Goguet, S. Shekhtman, C. Hardacre, R. Burcha, W. Deng and M. Flytzani-Stephanopoulos, *J. Catal.*, 2007, **247**, 269.
11. F. C. Meunier, D. Tibiletti, A. Goguet, S. Shekhtman, C. Hardacre and R. Burch, *Catal. Today*, 2007, **126**, 143.
12. G. Kresse and J. Hafner, *Phys. Rev. B*, 1993, **47**, 558.
13. G. Kresse and J. Hafner, *Phys. Rev. B*, 1994, **49**, 14251.
14. G. Henkelman, B. P. Uberuaga and H. Jónsson, *J. Chem. Phys.*, 2000, **113**, 9901.
15. V. M. Bermudez, *Chem. Phys.*, 2006, **323**, 193.
16. C. Binet, M. Daturi and J.-C. Lavalley, *Catal. Today*, 1999, **50**, 207.
17. G. Busca and V. Lorenzelli, *Mater. Chem.*, 1982, **7**, 89.
18. K. Pokrovski, K. T. Jung and A. T. Bell, *Langmuir*, 2001, **17**, 4297.
19. S. T. Korhonen, M. Calatayud and A. O. I. Krause, *J. Phys. Chem. C*, 2008, **112**, 16096.
20. S. E. Collins, M. A. Baltanas and A. L. Bonivardi, *Langmuir*, 2005, **21**, 962.
21. M. Calatayud, A. Markovits, M. Ménétrey, B. Mguig and C. Minot, *Catal. Today*, 2003, **85**, 125.
22. M. Calatayud, A. Markovits and C. Minot, *Catal. Today*, 2004, **89**, 269.
23. *NIST Computational Chemistry Comparison and Benchmark Database*, NIST Standard Reference Database Number 101, USA, release 12, August 2005, ed. Russell D. Johnson III, http://srdata.nist.gov/cccbdb/default.htm.
24. S. E. Collins, M. A. Baltanas and A. L. Bonivardi, *J. Phys. Chem. B*, 2006, **110**, 5498.
25. A. Bandara, J. Kubota, A. Wada, K. Domen and C. Hirose, *J. Phys. Chem. B*, 1997, **101**, 361.
26. K. K. Bando, K. Sayama, H. Kusama, K. Okabe and H. Arakawa, *Appl. Catal. A: General*, 1997, **165**, 391.
27. V. Boiadjiev and W. T. Tysøe, *Chem. Mater.*, 1998, **10**, 334.
28. G. Millar, C. Rochester and K. Waugh, *J. Catal.*, 1995, **155**, 52.
29. G. Busca, J. Lamotte, J.-C. Lavalley and V. Lorenzelli, *J. Am. Chem. Soc.*, 1987, **109**, 5197.

30. D. Clarke and A. T. Bell, *J. Catal.*, 1995, **154**, 314.
31. R. Fornika, E. Dinjus, H. Gorls and W. Leitner, *J. Organomet. Chem.*, 1996, **511**, 145.
32. D. H. Gibson, *Coord. Chem. Rev.*, 1999, **335**, 185.
33. P. G. Gopal, R. L. Schneider and K. L. Watters, *J. Catal.*, 1987, **105**, 366.
34. V. Grushin, C. Bensimon and H. Alper, *Organometallics*, 1995, **14**, 3259.
35. E. Guglielminotti, E. Giaello, F. Pinna, G. Strukul, S. Martinengo and L. Zanderighi, *J. Catal.*, 1994, **146**, 422.
36. M. Haneda, N. Bio, M. Daturi, J. Saussey, J.-C. Lavalley, D. Duprez and H. Hamada, *J. Catal.*, 2002, **206**, 114.
37. M. Hara, M. Kawamura, J. Kondo, K. Domen and K. Manuya, *J. Phys. Chem. B*, 1996, **100**, 14462.
38. F. Le Peltier, P. Chaumette, J. Saussey, M. M. Bettahar and J.-C. Lavalley, *J. Mol. Catal. A*, 1997, **122**, 131.
39. X. Mugniery, T. Chafik, M. Primet and D. Bianchi, *Catal. Today*, 1999, **52**, 15.
40. J. M. Phillips, F. Leibsle, A. J. Holder and T. Keith, *Surf. Sci.*, 2003, **545**, 1.
41. H. Uetsuka, M. A. Henderson, A. Sasahara and H. Onishi, *J. Phys. Chem. B*, 2004, **108**, 13706.
42. G. Busca, *Catal. Today*, 1996, **27**, 457.
43. J. Weigel, R. A. Koeppel, A. Baiker and A. Wokaun, *Langmuir*, 1996, **12**, 5319.
44. Y. Uemura, T. Taniike, M. Tada, Y. Morikawa and Y. Iwasawa, *J. Phys. Chem. C*, 2007, **111**, 16379.